

The Fractography of Thermoplastic Textile Fibres

J. W. S. HEARLE, P. M. CROSS

Department of Textile Technology, University of Manchester Institute of Science and Technology, U K

The use of a scanning electron microscope in studying the fractography of fibres is described and its advantages explained. A common pattern of break is shown for thermoplastic fibres at extension rates up to $8 \times 10^{-2} \text{ sec}^{-1}$. This involves a slow crack which becomes catastrophic at the critical crack length. The critical crack length depends upon the rate of extension, and possibly other undetermined factors. Under some conditions other forms of break are observed in thermoplastic fibres. A qualitative interpretation of the fracture phenomena is proposed.

1. Introduction

The technique of scanning electron microscopy, increasingly being used in fractography in general, is particularly useful when applied to fibre fractography, since the details are too small to be resolved in the optical microscope and the thin sectioning or replication needed to use transmission microscopy is extremely difficult with soft and fragile samples such as fibres. Magnifications using a scanning electron microscope (SEM) commonly run from $\times 20$ to $\times 50\,000^*$. The specimen holder is capable of all six degrees of freedom. Features of fracture may thus be viewed at optimum magnification, position, and direction, and are easily related to the whole fracture surface. It is found that, even with the very high depth of focus given by SEM, the actual shape of the fracture surface is not always clear until several views around the fibre have been taken; stereopairs are also helpful in building up a mental 3-D image of the complex form of the surface. In the pictures given in this paper, however, only one view of each fibre is given because of space restrictions.

2. Experimental Methods

Work has been done on a variety of fibres broken by different methods. In this paper we are specifically discussing the tensile failure of non-degraded thermoplastic fibres broken at normal rates of extension on an Instron tester, but some pictures of other types of fibre tensile break are

shown. The number of illustrations is limited to those needed to point out important aspects of the results. The comments made have been reinforced by repetitive tests on other fibres broken in a similar way, and by the more extensive examination of each break, which is possible though not conveniently publishable. The method of preparation of the samples for examination is relatively simple. As we wished to examine the fibre from all angles it was mounted vertically in a specially designed clamp on a modified Stereoscan stub, as shown in fig. 1. A semicircular metal block, pivoted about a pin, is pressed against a fixed block by the action of a spring. The interface between the two blocks lies accurately along one diameter of the stub and a line is scored on both blocks at the centre of the stub at right angles to this diameter. The moving block is pressed open, the fibres inserted vertically at the centre into the gap and the moving block allowed to swing back, gripping the fibre. Fibres of 15 denier (0.02 mm diameter) and upwards can be handled by fine tweezers, but finer fibres are picked up on adhesive tape and the whole assembly mounted in the clamp. The latter procedure has the advantage of easier handling and also gives the fibre rigidity and decreases its movement in the specimen chamber.

The fibre and clamp are placed in an evaporating unit and a layer of conductive material evaporated onto them. We used silver, since although it has a lower electron emission than

*Based on a screen size 10 cm \times 10 cm.

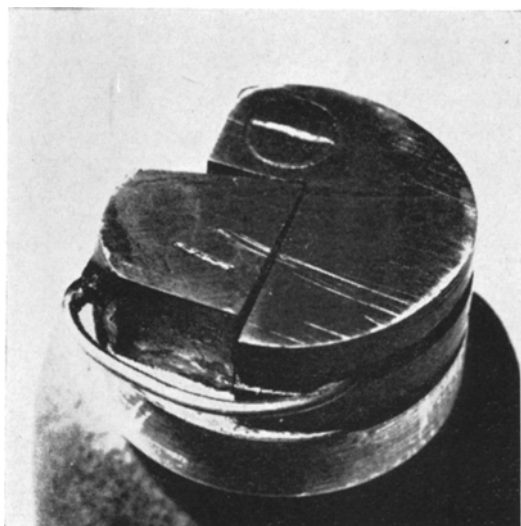


Figure 1 Fibre clamp.

the usual gold-palladium, it has better "contouring" behaviour, as shown by Tolansky [1].

3. Results

The first fibres studied were large (1 mm diameter) bristles of undrawn nylon 66, and these gave easily studied fracture surfaces most of whose features were found again in 15 denier (0.02 mm diameter) nylon 66, nylon 6, polypropylene and polyester fibres. These features were not seen on cotton, wool, viscose rayon or acrylic fibres, or on thermoplastic fibres broken at high rates of extension or after degradation.

3.1. Break of a Coarse Bristle of Nylon 66

The undrawn bristles of diameter 1 mm were tested to fracture in an Instron tensile tester at $8 \times 10^{-4} \text{ sec}^{-1}$, $8 \times 10^{-3} \text{ sec}^{-1}$ and $8 \times 10^{-2} \text{ sec}^{-1}$ strain rates. The sequence of events was that a

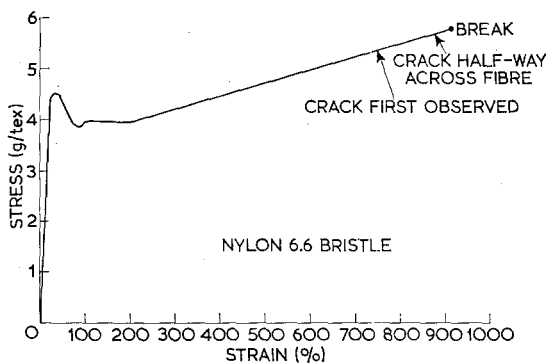


Figure 2 Load extension graph of nylon 66 bristle.

*All magnifications quoted in figure captions refer to the instrument magnification with a screen size of 10 cm \times 10 cm.

length of bristle (usually 1 cm) was clamped in the tester and extended. The load extension behaviour is shown in fig. 2. Initially there was a uniform deformation under steadily increasing load, then a neck developed and the load dropped. The drawn portion grew until the total extension was several hundred per cent and the specimen was again uniform. Further extension proceeded at a load which increased slowly and uniformly until it fell abruptly to zero at the final rupture of the specimen. Long before this occurred a faint crack had become just visible in the specimen; this grew into a well-developed notch with the appearance indicated in fig. 3. The notch had extended a considerable distance through the fibre before the final rupture. Figs. 4 and 5 show two fractured ends of such a fibre



Figure 3 Appearance of notch in fibre before failure.

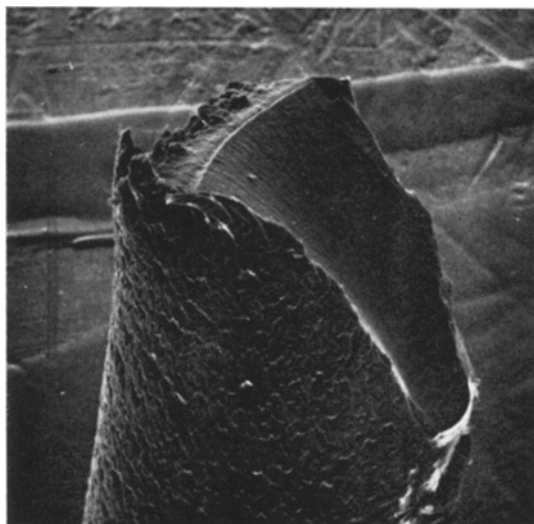


Figure 4 End A of nylon 66 bristle fractured at $8 \times 10^{-4} \text{ sec}^{-1}$ ($\times 52$).*

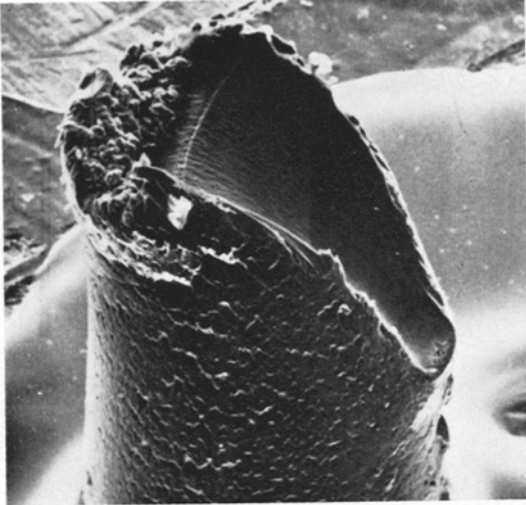


Figure 5 End B of nylon 66 bristle fractured at $8 \times 10^{-4} \text{ sec}^{-1}$ ($\times 50$).

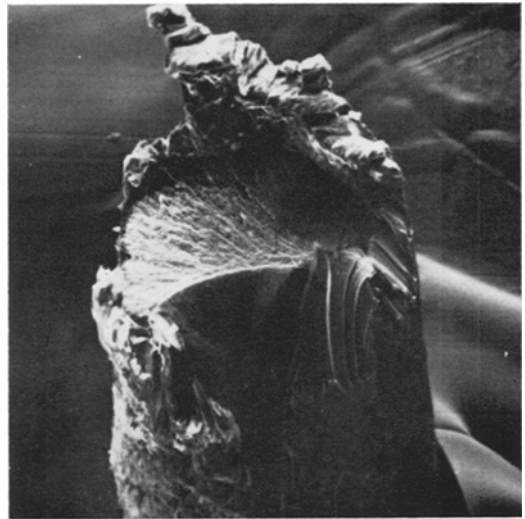


Figure 6 End A of nylon 66 bristle fractured at $8 \times 10^{-3} \text{ sec}^{-1}$ ($\times 52$).

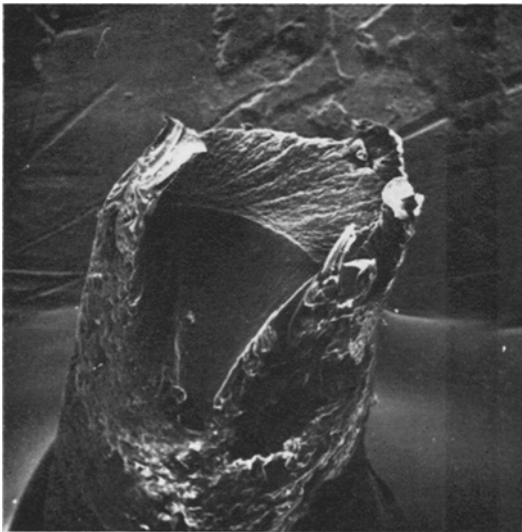


Figure 7 End B of nylon 66 bristle fractured at $8 \times 10^{-3} \text{ sec}^{-1}$ ($\times 52$).

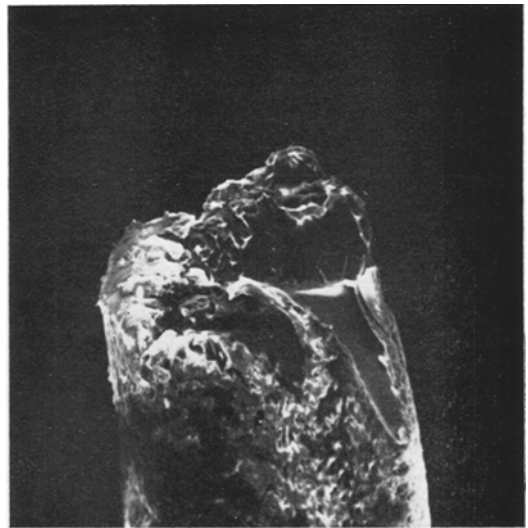


Figure 8 End A of nylon 66 bristle fractured at $8 \times 10^{-2} \text{ sec}^{-1}$ ($\times 50$).

extended at $8 \times 10^{-4} \text{ sec}^{-1}$, figs. 6 and 7 are similar pictures where the fibre has been extended at $8 \times 10^{-3} \text{ sec}^{-1}$ and figs. 8 and 9 where the fibre has been extended at $8 \times 10^{-2} \text{ sec}^{-1}$. It can be seen that there are five main regions on each break, indicated in position on fig. 10.

- (i) The crack initiation region A.
- (ii) Region B, a smooth cupped region rising from the surface of the fibre, at the crack initiation point, to somewhere in the interior of the fibre.
- (iii) Region C, a series of sharp steps, concentric

with the initiation point.

- (iv) Region D, a less smooth region, perpendicular to the fibre axis.
- (v) Region E, a very rough area at the edge of the fibre.

Region B dominates the fibres broken more slowly but region D begins to become important as the rate of extension rises. If we look at the two ends of the same fibre we see that regions A and B on the two ends are mirror images of one another but regions D and E mate; this is particularly obvious in figs. 6 and 7. The five regions

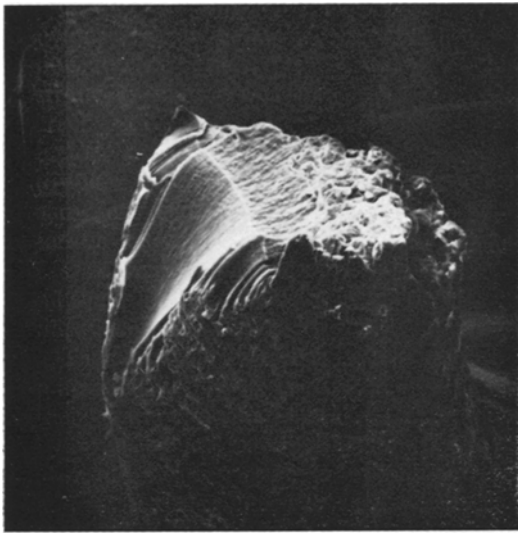


Figure 9 End B of nylon 66 bristle fractured at 8×10^{-2} sec⁻¹ ($\times 60$).

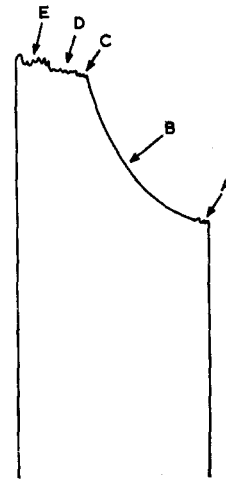


Figure 10 Diagrammatic representation of fracture surface of bristle.

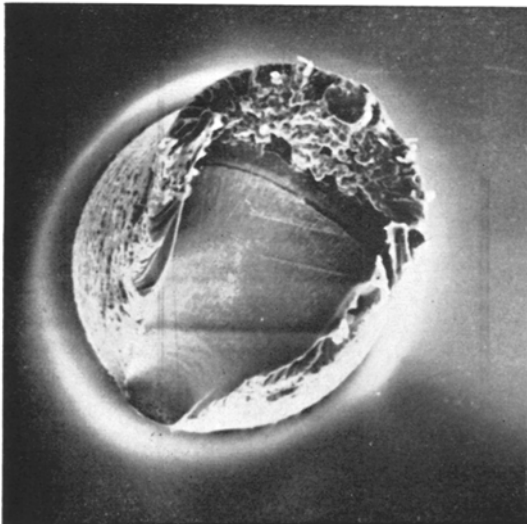


Figure 11 Plan view of fractured bristle ($\times 47$).

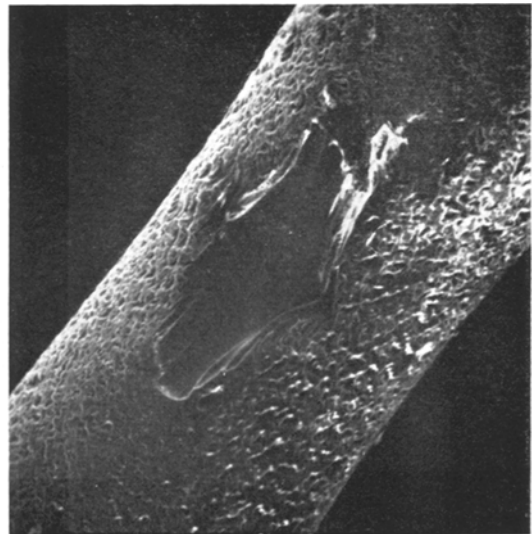


Figure 12 Micrograph of cracked bristle ($\times 50$).

have the same character in each break and so photographs which show the features of the regions most clearly, not necessarily taken from the same fibre, will be shown.

We consider region B to be an area of slow tearing while cold-drawing continues in the uncracked part of the fibre. This view is upheld by the reduction in diameter of the fibre in this region (see fig. 11) and by a picture of a crack just starting (fig. 12). If one looks at the region A (fig. 13) it can be seen that there is a honeycomb

effect, probably caused by internal cavitation before fracture. The cavitation becomes smaller further along the crack, and there are markings which might be secondary crack fronts.

At some point the energy supplied to the decreased area of the fibre is too great to be absorbed by the slow cracking and drawing of the fibre, and slip-stick occurs (region C) as shown in detail in fig. 14. This is quickly followed by a fast fracture at region D (fig. 15), the markings on the surface indicating whether the frac-

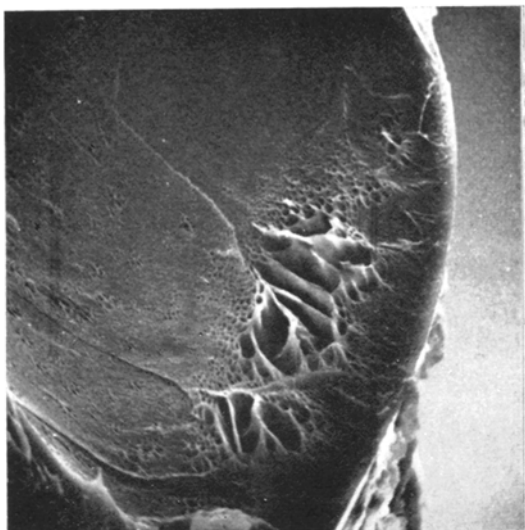


Figure 13 Region A of fractured bristle ($\times 485$).

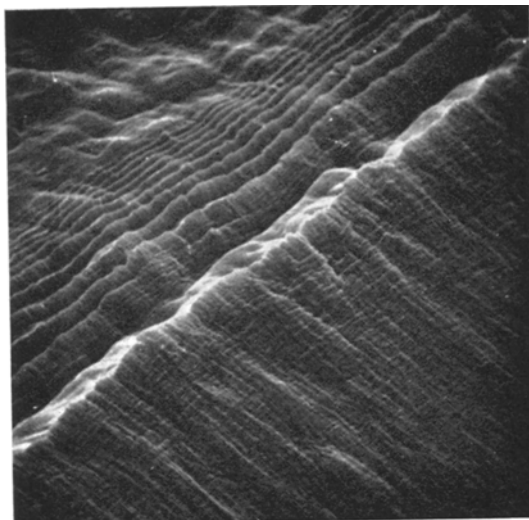


Figure 14 Region C of fractured bristle ($\times 1015$).

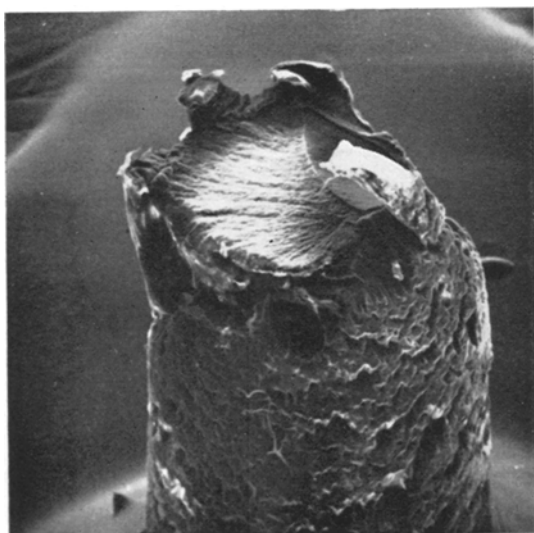


Figure 15 Region D of fractured bristle ($\times 55$).

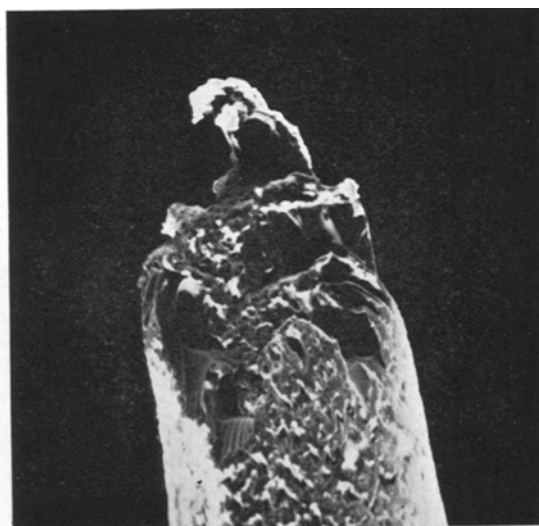


Figure 16 Nylon 66 bristle fractured at $8 \times 10^{-2} \text{ sec}^{-1}$ showing several initiation sites ($\times 48$).

ture is still taking place concentrically around the initiation point or whether it changes its angle after the slip-stick. At the very edge of the fibre, extensive tearing and ripping takes place (region E).

It is worth pointing out that when the fracture takes place at a high rate of extension these processes often occur at several sites on the fibre (fig. 16).

3.2. Break of 15 Denier Drawn Nylon 66 Fibres

Drawn nylon fibres (approximately 0.02 mm in

diameter) were broken in an Instron tester at the same rates as the bristles, and show the same general features as they do, except for the absence of region C, which becomes a sharply defined line, the line of catastrophe, or, quite often, a single step. Fig. 17 shows a fibre broken at $8 \times 10^{-4} \text{ sec}^{-1}$. In this, and other pictures, only one end is shown, but both ends were examined, and, as before, regions A and B are mirror images while regions D and E mate. There is considerable radial ridging on region B and a line of holes around the edge of this region, but no honeycombing at region A. The absence of

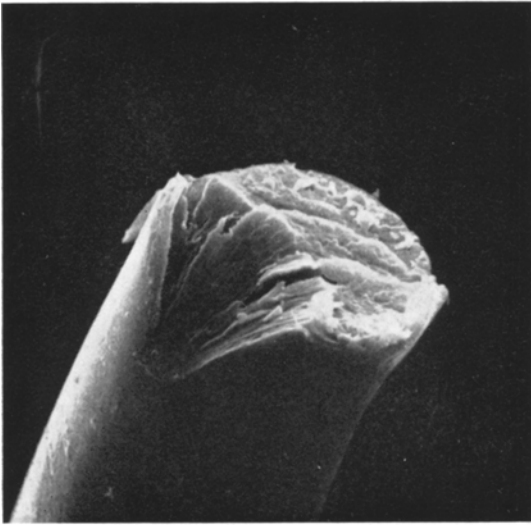


Figure 17 15 denier nylon 66 fractured at $8 \times 10^{-4} \text{ sec}^{-1}$ ($\times 700$).

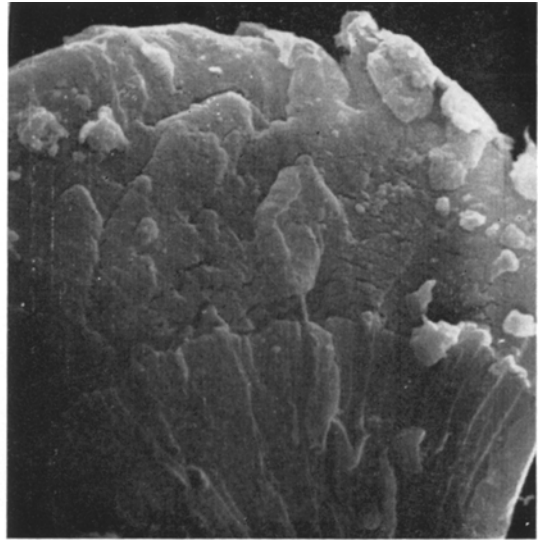


Figure 18 Detail of fig. 17 ($\times 1500$).

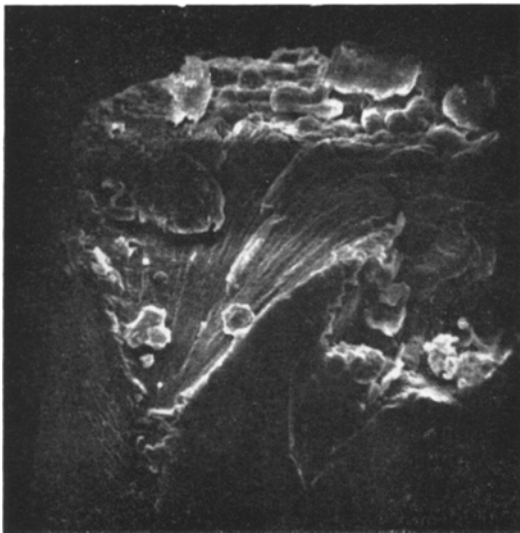


Figure 19 15 denier nylon 66 fractured at $8 \times 10^{-3} \text{ sec}^{-1}$ ($\times 1050$).

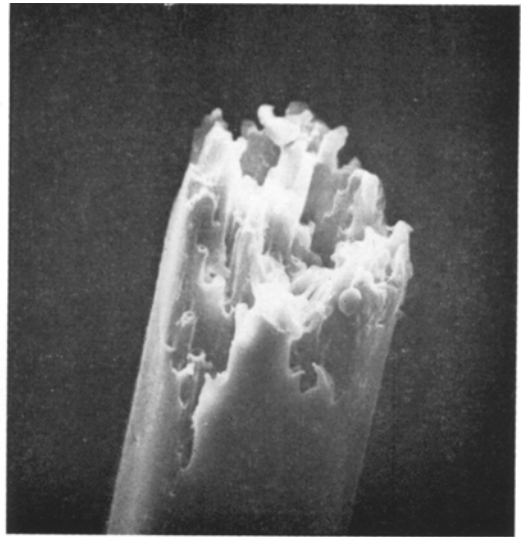


Figure 20 Fracture surface of a light-degraded nylon 66 15 denier fibre ($\times 360$).

region C is clearly shown in fig. 18. Fig. 19 shows unusual features in a fibre broken at $8 \times 10^{-3} \text{ sec}^{-1}$. There are two B-type regions here, suggesting double initiation, and a curious "wrinkled skin effect" on the surface of the fibre around region A. The effect of changing the rate of extension is not so marked as it was with the bristles.

In fig. 20 the fractured surface of a light-degraded 15 denier nylon 66 is shown. It is spectacularly different from the other fracture

surfaces. When nylon is exposed to light for a few weeks it becomes badly cavitated and suffers a loss in strength. No clear fracture path is visible; the weak points caused by holes seem to have simply broken in a brittle manner. This picture is probably indicative of the internal microstructure of light-degraded nylon and it is interesting to note that the order of magnitude of the diameter of the "turrets" is the same as the width of the ridges in region A of the tensile breaks of 15 denier nylon—a few microns.



Figure 21 15 denier nylon 6 fibre (strain rate $8 \times 10^{-4} \text{ sec}^{-1}$) at breaking extension of 39% ($\times 680$).

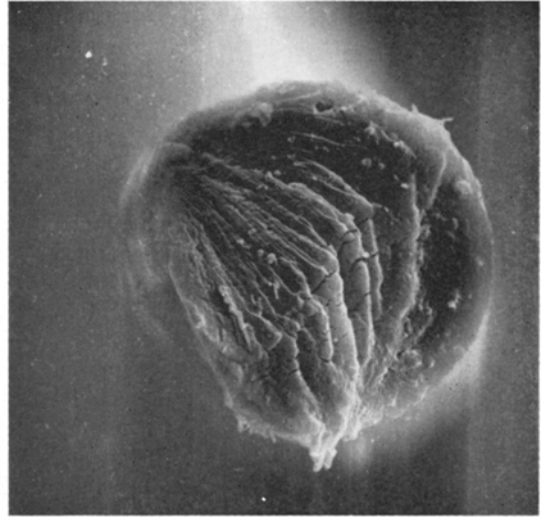


Figure 22 15 denier nylon 6 fibre (strain rate $8 \times 10^{-3} \text{ sec}^{-1}$) at breaking extension of 43% ($\times 750$).

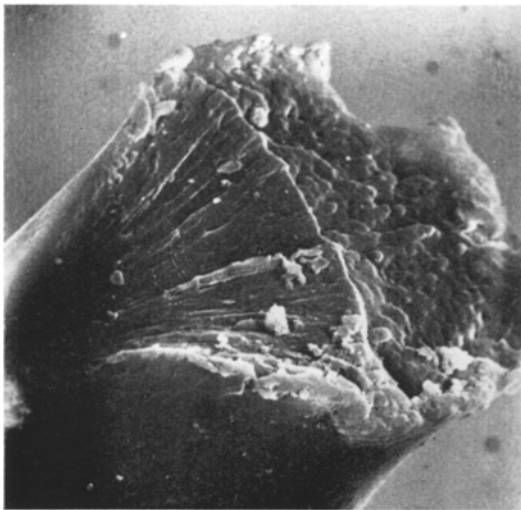


Figure 23 15 denier nylon 6 fibre (strain rate $8 \times 10^{-3} \text{ sec}^{-1}$) at breaking extension of 37.5% ($\times 1030$).

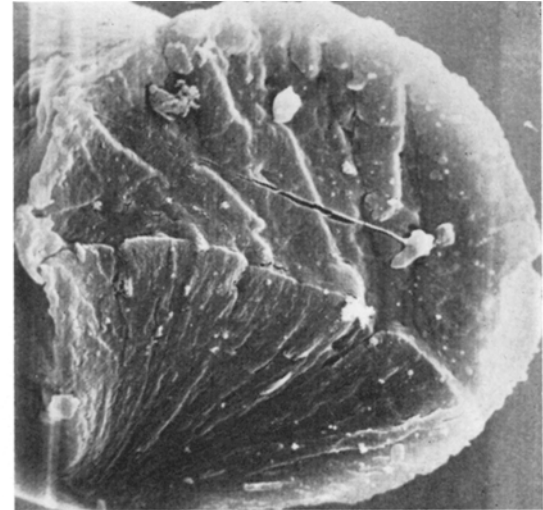


Figure 24 15 denier nylon 6 fibre (strain rate $8 \times 10^{-3} \text{ sec}^{-1}$), at breaking extension of 56% ($\times 1020$).

3.3. Drawn 15 Denier Nylon 6 Fibres

The relationship between the two ends is as before. The same general pattern of break is seen with ridging on region B and ridging on some fibres on region D at about 45° to the line of catastrophe. The latter effect seems to be associated with a larger extension to break. At small extension to break, rounded features predominate on region D with fibrous effects on and between them. (Fig. 21 gives an example of this.) There is also considerable cracking.

Fig. 21 shows a fibre broken at a strain rate

$8 \times 10^{-4} \text{ sec}^{-1}$, at a breaking extension of 39%; a similar fibre which broke at 43% is shown in fig. 22. Figs. 23 and 24 show nylon 6 fibres broken at $8 \times 10^{-3} \text{ sec}^{-1}$; in fig. 23 the breaking extension was 37.5% and in fig. 24, 56%. Fig. 25 shows a fibre broken at $8 \times 10^{-2} \text{ sec}^{-1}$; the breaking extension is 42.5%.

3.4. 3 Denier Polyester

Some studies of polyester fibres showed breaks that were generally similar to those of nylon, though region E was more pronounced.

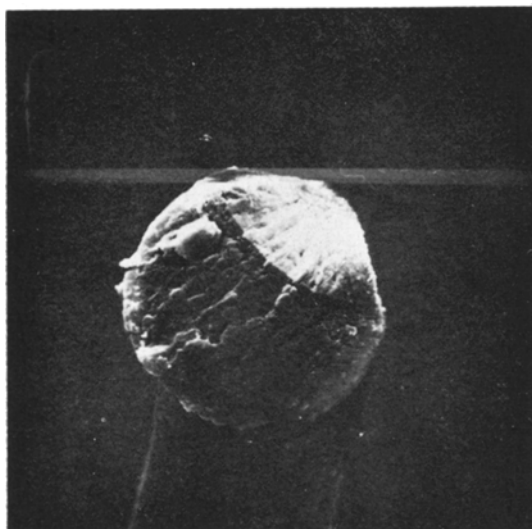


Figure 25 15 denier nylon 6 fibre (strain rate $8 \times 10^{-2} \text{ sec}^{-1}$), at breaking extension of 42.5% ($\times 550$).

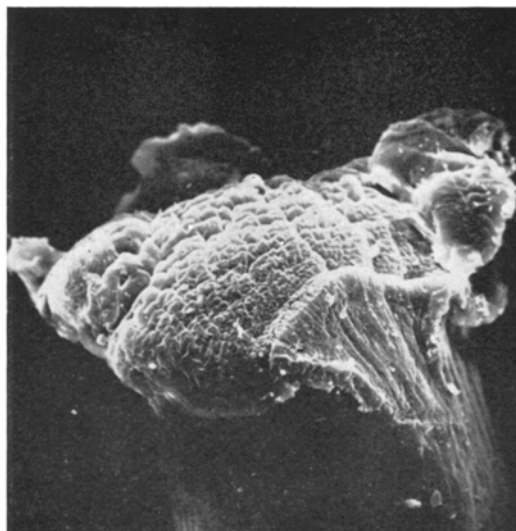


Figure 26 End A of 30 denier polypropylene fibre broken at $5 \times 10^{-3} \text{ sec}^{-1}$ strain rate ($\times 330$).



Figure 27 Another view of fibre in fig. 26 ($\times 260$).

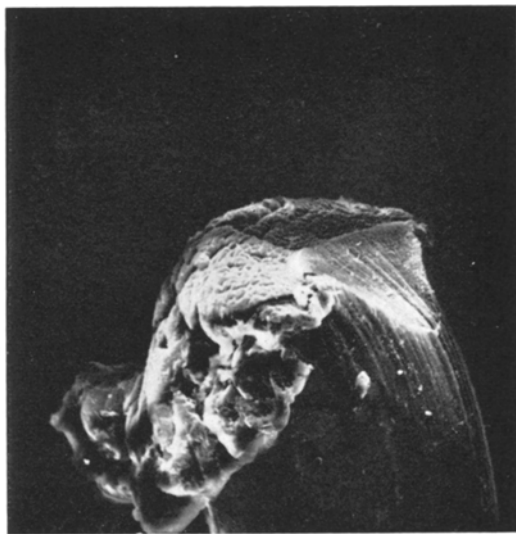


Figure 28 End B of fibre in fig. 26 ($\times 275$).

3.5. Break of 30 Denier Polypropylene

Drawn polypropylene approximately 0.04 mm in diameter was fractured at $5 \times 10^{-3} \text{ sec}^{-1}$ and 5 sec^{-1} rates of extension in a tensile tester. Figs. 26 and 27 are two views of one end of a fibre broken at $5 \times 10^{-3} \text{ sec}^{-1}$ and fig. 28 is a view of the other end of the fracture. Region B is here, as usual, ending at the line of catastrophe, but the cobbled effect of region D and the overhang into which region E is converted, appear to be peculiar to polypropylene. Figs. 29 and 30 are two views of one end of a fibre broken at 5 sec^{-1}

extension rate; fig. 31 shows the other end. The two ends appear to have little relation to one another and none to the type of fracture seen at lower extension rates. One end appears to have been pinched in by the fracture and the other end to have been mushroomed out. More detailed work on this change in fracture mode is proceeding and will be published soon.

4. Conclusions

The general sequence of events in the rupture of the coarse bristles is fairly clear, and this is

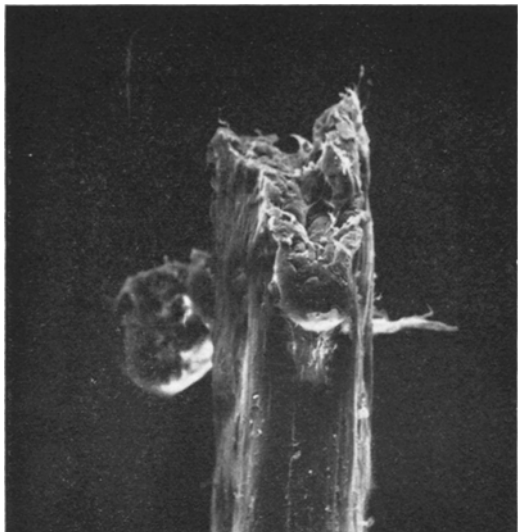


Figure 29 End A of 30 denier polypropylene fibre broken at 5 sec^{-1} strain rate ($\times 240$).

followed, with some modifications, by the textile fibres, although there are obviously some possibilities of divergence and complication. These thermoplastic fibres, broken in tension at rates up to at least $8 \times 10^{-2} \text{ sec}^{-1}$ at room temperature and normal humidity, follow a common pattern of break.

As the specimen is stressed up to near its breaking point, internal cracks or voids grow in size by stable propagation until they coalesce. Apparently, and the reasons for this may be a structural difference, or some more general

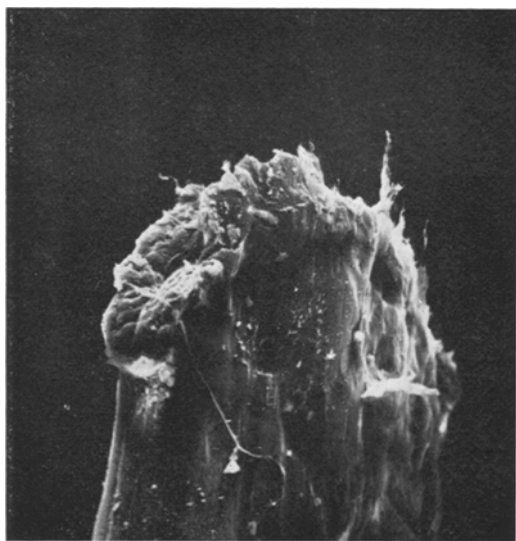


Figure 30 Another view of fibre in fig. 29 ($\times 238$).

mechanism, this happens first near the surface to give the initiation region A. Stable crack growth then proceeds as the specimen is further extended. Eventually a catastrophic situation develops, either because crack propagation becomes unstable or because the stress in the small area left opposite the crack becomes so high that internal voids become unstable and lead to failure. The roughness of region D in the undrawn bristle tends to indicate the latter mechanism. A different mechanism probably accounts for the smoothness of region D in polypropylene.

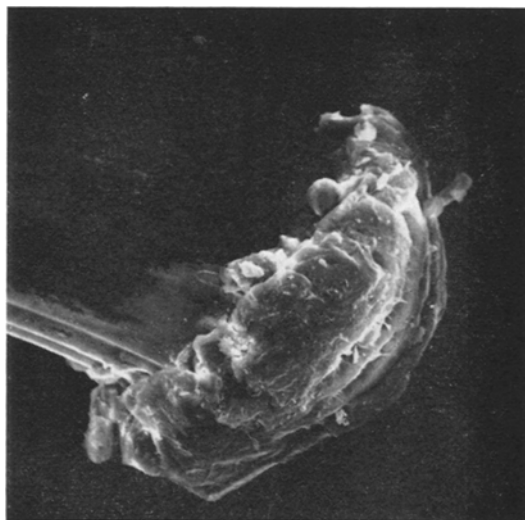


Figure 31 End B of fibre in fig. 29 ($\times 250$).

On the surface, the crack appears as a diamond-shaped flaw as observed in the optical microscope by Chadwick and Simmens [2]. As the load increases and the crack grows, the fibre continues to draw and the open fracture surface is forced to lie obliquely to the fibre axis. There is little increase of load needed to continue drawing the fibre during the period of crack growth. So this mode of failure explains Moseley's [3] observation that the tenacity of nylon and polyester fibres at room temperature equals their primary yield stress, and that there is no loss in strength as a result of putting a 1 mil nick into an 8 mil nylon fibre.

However, if flaws, which lead to the initiation of cracking, could be eliminated it should be possible to draw the fibres to a greater extent and secure a higher strength. Certainly the stress taken by the unbroken portion opposite a crack just before catastrophic failure must be much higher than reported fibre strengths. The critical

crack length depends on the rate of extension and probably upon other factors such as temperature, humidity and degree of orientation within the fibre. It is proposed to study the detailed effect of those factors on one specific fibre in the future. Non-thermoplastic fibres do not show the same pattern of events at these rates of extension, nor do degraded thermoplastic fibres or those extended at high speeds.

In the light-degraded nylon, the high tensile stress parallel to the crack direction (perpendicular to the main tensile stress) just ahead of the crack, as discussed by Cook and Gordon [4], presumably leads to failure in a region of de-

gradation and prevents the continued crack propagation. The break splits up into a series of separate turrets.

References

1. S. TOLANSKY, *Vacuum* **4** (1954) 456.
2. G. E. CHADWICK and S. C. SIMMENS, *J. Textile Inst.* **52** (1961) 40.
3. W. W. MOSELEY, *J. Appl. Polymer Sci.* **7** (1963) 187.
4. J. COOK and J. E. GORDON, *Proc. Roy. Soc.* **A282** (1964) 508.

Received 23 January and accepted 2 March 1970.